POLYHEDRAL OXARUTHENABORANE CHEMISTRY. CHARACTERISATION OF A $[(\eta^6\text{-}C_6Me_6)RuOB_9H_{13}]$ SPECIES OF *arachno* ELEVEN-VERTEX CLUSTER CHARACTER AND OTHER ASPECTS OF OXABORANE CHEMISTRY

Jonathan BOULD[1], Mark BOWN[2] and John D. KENNEDY[3,*]

The School of Chemistry of the University of Leeds, Leeds, UK LS2 9JT, England; e-mail: [1] bould@chem.leeds.ac.uk, [2] mark.bown@csiro.au, [3] johnk@chem.leeds.ac.uk

Received January 18, 2005
Accepted March 23, 2005

$[(\eta^6\text{-}C_6Me_6)RuOB_9H_{13}]$, obtained in trace yield from the reaction between $[\{RuCl_2(\eta^6\text{-}C_6Me_6)\}_2]$ and the [*arachno*-$B_6H_{11}]^-$ anion, has been shown by DFT calculations of structure and of boron-atom nuclear shielding to be of an *arachno* eleven-vertex cluster geometry that is derived by the removal of adjacent six-connected and five-connected vertices from a closed thirteen-vertex deltahedral 1:6:5:1 stack. The results lead to further considerations in oxaborane chemistry, which are explored and consolidated by calculation. Additional products from the reaction include [4-$(\eta^6\text{-}C_6Me_6)$-*n*-*arachno*-4-RuB_8H_{14}], also substantiated by DFT calculations, and several four-, five-, six-, nine- and ten-vertex ruthenaboranes that are either known compounds or simple variants of known compounds.

Keywords: Borane cluster; Oxaboranes; Oxametallaboranes; DFT calculations; Ruthenaboranes; Metallaboranes; Crystal structure; X-ray diffraction.

Polyborane-based boron-containing cluster compounds that also contain oxygen as a cluster constituent are rare, although the few examples that are known are generally stable and can be readily manipulated in the laboratory without recourse to rigorous anaerobic techniques. The known examples are limited to two oxaborane anions, specifically the nineteen-vertex $[OB_{18}H_{21}]^-$ anion (species **1**) (schematic cluster structure **I**), in which the oxygen atom has a cluster connectivity-number of two[1], and the *nido*-type twelve-vertex $[OB_{11}H_{12}]^-$ anion **2** (schematic cluster structure **II**), in which the oxygen atom has a cluster connectivity-number of three[2–6], together with four neutral oxametallaboranes in all of which the oxygen atom has a cluster connectivity-number of three[6–10].

These last four consist of *nido*-type twelve-vertex $[(\eta^5\text{-}C_5Me_5)RhOB_{10}H_9Cl(PMe_2Ph)]$ **3** (schematic cluster structure **III**)[6,7] and $[(\eta^5\text{-}C_5Me_5)RhOB_{10}H_{10}(NEt_3)]$ **4** (schematic cluster structure **IV**)[6,8], both closely related to anion **2**

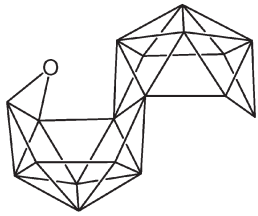

I

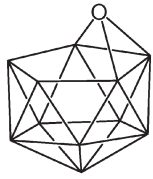

II

(schematic **II**), *nido* ten-vertex [(η^6-$C_6H_3Me_3$)$FeOB_8H_{10}$] **5** (schematic cluster structure **V**)[9], and *arachno*-type ten-vertex [$(PMe_2Ph)_2PtOB_8H_{10}$] **6** (schematic cluster structure **VI**)[10]. We now report the isolation and characterisation of a new oxametallaborane, a species of formulation [(η^6-C_6Me_6)- $RuOB_9H_{13}$] **7**, that has a new eleven-vertex *arachno*-type cluster geometry (schematic cluster structures **VII A** and **VII B**) and that also exhibits an oxygen-to-cluster connectivity-number of three.

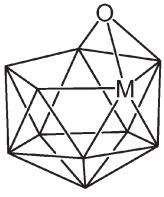

III

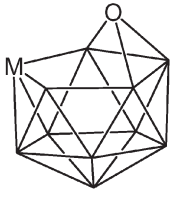

IV

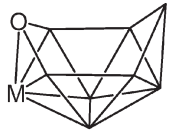

V

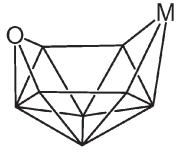

VI

RESULTS AND DISCUSSION

Some time ago we reported the species [1-(η^6-C_6Me_6)-*nido*-1-RuB_9H_{13}] **8** (*nido* ten-vertex numbering system) (Fig. 1 (left), schematic cluster structure **VIII**) as a yellow crystalline solid[11], characterised by single-crystal X-ray diffraction analysis and NMR spectroscopy. Of formal *nido* ten-vertex {MB_9} cluster constitution, the solid-state molecular structure exhibits an anomalously long B(5)–B(10) interatomic distance of 2.497(7) Å. This distance is well outside bonding range, and gives compound **8** a much more open cluster aspect than is commonly associated with the ten-vertex *nido*-decaboranyl constitution. For example, its 2-isomer, [2-(η^6-C_6Me_6)-*nido*-2-RuB_9H_{13}] **9** (schematic cluster structure **IX**), has a much shorter interboron distance of 1.96(1) Å for the equivalent site[11], comparable to that in *nido*-$B_{10}H_{14}$ itself of 1.973(4) Å [12].

VII A VIII IX

The NMR characteristics of compound **8** (Table I) are in accord with the crystallographically determined *nido* ten-vertex cluster structure. Compound **8** can be obtained, albeit in modest yields of ca. 9%, from the reaction of $[\{RuCl_2(\eta^6\text{-}C_6Me_6)\}_2]$ either with the *nido* five-vertex $[B_5H_8]^-$ anion[11], or with the *arachno* six-vertex $[B_6H_{11}]^-$ anion as described below. From the second of these two reactions, viz. the reaction between $[\{RuCl_2(\eta^6\text{-}C_6Me_6)\}_2]$ and the $[\textit{arachno}\text{-}B_6H_{11}]^-$ anion followed by chromatographic separation and purification in air, we now report the isolation of trace quantities (ca. 0.2% yield) of an interestingly related species **7**, also a deep yellow crystalline solid, of formulation $[(\eta^6\text{-}C_6Me_6)RuOB_9H_{13}]$. NMR spectroscopic experiments carried out on solutions of compound **7** (Table I and Fig. 2) indicate the same $\{(\eta^6\text{-}C_6Me_6)RuB_9H_{13}\}$ content, connectivity and symmetry as that of $[1\text{-}(\eta^6\text{-}C_6Me_6)\text{-}\textit{nido}\text{-}1\text{-}RuB_9H_{13}]$ **8**, but the ^{11}B and ^1H chemical shifts of the $\{B_9H_{13}\}$ cluster unit are quite differently ordered, and the mean ^{11}B nuclear shielding of the cluster boron atoms differs by some 16 ppm per atom site. Mass spectrometry gave a molecular ion for **7** that is 16 mass units in excess of a $\{(\eta^6\text{-}C_6Me_6)RuB_9H_{13}\}$ formulation, which in turn suggests the

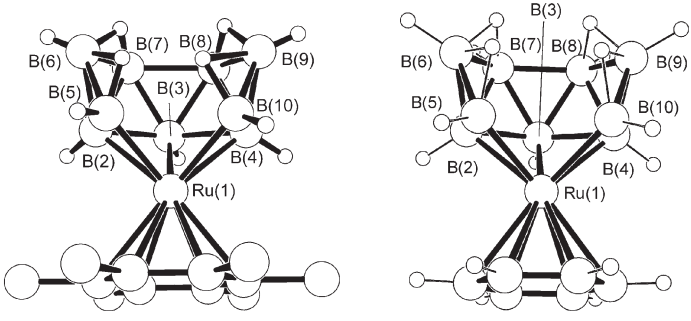

FIG. 1

Crystallographically determined molecular structure[11] for $[1\text{-}(\eta^6\text{-}C_6Me_6)\text{-}\textit{nido}\text{-}6\text{-}RuB_9H_{13}]$ **8** (left-hand diagram) and the calculated molecular structure (DFT; B3LYP/6-31G*) for $[1\text{-}(\eta^6\text{-}C_6H_6)\text{-}\textit{nido}\text{-}6\text{-}RuB_9H_{13}]$ **8A** (right-hand diagram). For selected dimensions see Table III. In the crystallographic solution for compound **8**, methyl hydrogen atoms were not located[11]

TABLE I
Measured ($CDCl_3$, 294–300 K) and calculated NMR chemical shifts $\delta(^{11}B)$ and $\delta(^1H)$ for $[(\eta^6\text{-}C_6Me_6)RuOB_9H_{13}]$ **7**

Position	NMR chemical shifts, ppm					
	$\delta(^{11}B)$		$\Delta\delta(^{11}B)$	$\delta(^1H)$		$\Delta\delta(^1H)$
	calculated	measured	difference	calculated	measured	difference
(2,4)	–24.8	–26.2	+1.6	+1.67	+1.09	+0.56
(3)	+28.6	+26.1	+2.5	+4.39	+3.65	+0.79
(5,10)	+11.2	+14.0	–2.8	+3.80	+3.41	+0.39
(6,9)	–23.9	–25.7	+1.8	+2.13	+1.49	+0.64
(7,8)	–16.0	–16.5	+0.5	+2.20	+1.79	+0.40
(5,6;9,10)	–	–	–	+0.38	+0.15	–0.25
(6,7;8,9)	–	–	–	–5.25	–5.64	–0.39
C_6Me_6	–	–	–	+2.05	+2.15	–0.10

oxide formulation $[(\eta^6\text{-}C_6Me_6)RuOB_9H_{13}]$. This conclusion is also consistent with high-resolution mass spectrometric experiments that gave values for the highest mass isotopomers of 394.22404 and 378.22987 Da for **7** and **8**, respectively, in reasonable correspondence with the calculated values of 394.225460 and 378.230456 Da, respectively. It thence seemed reasonable to postulate a structure related to that of **8**, but with an oxygen atom (i) that is contiguously bound to the cluster on the symmetry-plane through the metal atom, and (ii) that is associated with the metal atom and accommodated on the cluster open face within the B(5)–B(10) gap (*nido*-decaboranyl numbering) (schematic cluster structure **VII B**; see also **VII A** above and **VII C** below).

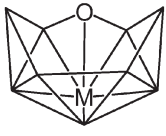

VII B

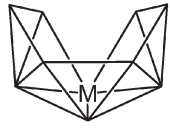

VIII

The few crystallographically confirmed single-cluster oxaborane skeletons that have been previously established also have their oxygen atoms in similar open-face positions of cluster-connectivity of three (schematics **II** to **VI** above)[7–10]. In particular there is a good parallel with the configuration about the metal–oxygen site in the *nido*-type ten-vertex species $[(\eta^6\text{-}(C_6H_3Me_3)FeOB_8H_{10}]$ (compound **5**)[9] (schematic cluster structure **V** above).

We have been able strongly to support the proposed formulation and structure of compound **7** by the use of DFT calculations of structure and thence of the nuclear magnetic shielding of the cluster boron atoms, of which the latter compare well with the experimentally observed $\delta(^{11}B)$ NMR chemical shift values. Thus we found that structural calculations at the B3LYP level of theory, using 6-31G* basis sets for C, H, B and O and the LANL2DZ basis set for ruthenium, indeed minimised at a structure of sche-

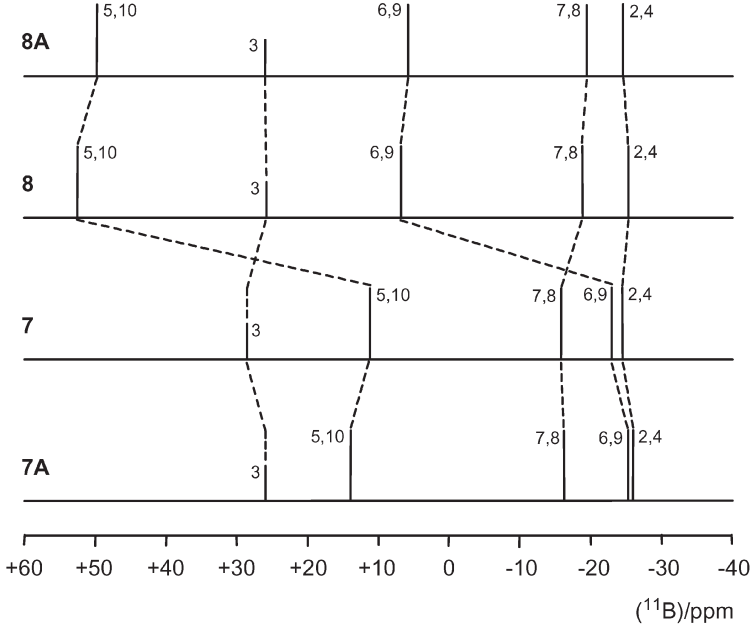

FIG. 2

Stick representations of the relative intensities and chemical shifts in ^{11}B NMR spectra, as calculated for $[(\eta^6\text{-}C_6H_6)RuB_9H_{13}]$ **8A** (top), as measured for $[(\eta^6\text{-}C_6Me_6)RuB_9H_{13}]$ **8** (upper centre), and as measured **7** (lower centre) and as calculated **7A** (bottom) for $[(\eta^6\text{-}C_6Me_6)RuOB_9H_{13}]$ (compound **7**). Hatched lines join equivalent positions in the two species

matic skeletal configuration **VII**, as illustrated in Fig. 3. Interestingly, in this calculated structure of the oxametallaborane **7**, the oxygen atom has in fact fitted very nicely into the {Ru(1)B(5)B(10)} cleft in compound **8**, with the B(5)–B(10) distances for **7** (calculated) and **8** (experimental) being similar at 2.656 and 2.497(7) Å, respectively. There is a more exact match with the calculated structure **8A**, rather than experimental structure, for the non-oxygenated compound **8** (see the next paragraph below), in that **8A** has a distance of 2.672 Å for the B(5)–B(10) separation. Here it may be noted that it is unlikely that small variations in the non-bonded B(5)–B(10) distance in the non-oxygenated species **8** will be energetically significant. In any event, GIAO nuclear shielding calculations on the calculated structure for **7** thence gave the calculated values of $\delta(^{11}B)$ as summarised in Table I. It can be seen that these closely mimic the observed values, tending to confirm the overall structural supposition.

To increase confidence in the validity of such calculations, we performed similar calculations for the non-oxygenated [1-(η^6-C_6Me_6)-*nido*-1-RuB_9H_{13}] compound **8**, using the [1-(η^6-C_6H_6)-*nido*-1-RuB_9H_{13}] analogue **8A** as a reasonable model, from which the calculated results for both the basic molecular structure and the ^{11}B nuclear shielding thence closely mimic those determined experimentally for **8** (Fig. 1 (right), Fig. 2 and Table II).

Also, because oxygen is now involved in the cluster, it was of interest to carry out similar calculations for the oxaplatinaborane [$(PMe_2Ph)_2$-$PtOB_8H_{10}$] **6** (Fig. 4 (left)), for which a crystallographically determined molecular structure and cluster ^{11}B NMR chemical shifts have been estab-

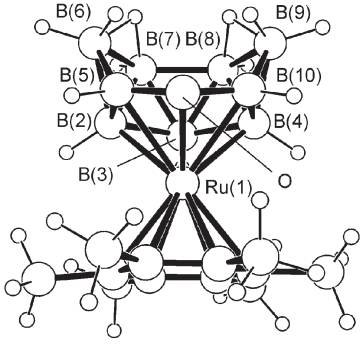

FIG. 3
Calculated (DFT; B3LYP/6-31G*) molecular structure for [(η^6-C_6Me_6)$RuOB_9H_{13}$] **7**. For ease of comparison, the numbering follows that in [1-(η^6-C_6Me_6)-*nido*-1-RuB_9H_{13}] **8**, rather than an *arachno* eleven-vertex numbering scheme. For selected dimensions see Table III

lished[10]. In this case, however, although the gross structure was reproduced (Fig. 4 (right)), there was some discrepancy, around the metal atom, between the calculated structure **6A** and the crystallographically determined structure **6**. Thus, in the calculated structure **6A**, the distances from Pt(9) to P(1), P(2) and B(4), respectively, at 2.395, 2.377 and 2.237 Å, were all significantly longer than the experimentally derived respective distances of 2.299(2), 2.300(2) and 2.198(7) Å. The rest of the structure, however, showed a close correspondence, particularly around the oxygen atom. The calculated boron nuclear shielding for the B(8,10) positions adjacent to the Pt(9) site was also significantly different from that measured experimentally (see caption to Fig. 4), with a value for $\delta(^{11}B)(8,10)$ of –15.7 calculated for **6A**, versus a value of –22.6 as measured for **6**. The other boron sites, including B(4) next to Pt(9), however, showed good agreement, with a maximum disagreement of 1.5 ppm. We have observed similar structural and magnetic shielding discrepancies for sites around the metal atom in test calculations with other quasi-square-planar $\{Pt(PR_3)_2\}$ borane species. Thus, for example, we have noted this type of behaviour in calculations of the boron nuclear shieldings on minimised structures for $[L_2PtB_8H_{12}]$, where L is a

TABLE II
Measured[a] NMR chemical shifts for [1-(η^6-C_6Me_6)-*nido*-6-RuB_9H_{13}] **8** and calculated shifts for [1-(η^6-C_6H_6)-*nido*-6-RuB_9H_{13}] **8A**

Position	NMR chemical shifts, ppm					
	$\delta(^{11}B)$		$\Delta\delta(^{11}B)$	$\delta(^{1}H)$		$\Delta\delta(^{1}H)$
	calculated	measured	difference	calculated	measured	difference
(2,4)	–24.5	–24.8	+0.3	+1.48	+0.16	+1.32
(3)	+26.4	+26.2	+0.2	+5.46	+4.29	+1.16
(5,10)	+49.8	+52.9	–3.1	+6.04	+5.07	+0.96
(6,9)	+5.7	+6.6	–0.7	+3.73	+3.54	+0.19
(7,8)	–19.0	–18.6	–0.4	+2.20	+1.66	+1.54
(5,6;9,10)	–	–	–	–2.77	–2.58	+0.19
(6,7;8,9)	–	–	–	–2.68	–2.49	+0.19
C_6Me_6	–	–	–	–	+2.11	–

[a] Measured data taken from lit.[11]; $CDCl_3$, 294–300 K.

triorganylphosphine ligand (unpublished observations). Other basis sets, or the inclusion of relativistic factors, may be more appropriate for such configurations of this third-row transition-element centre.

In any event, for further confidence we also performed these types of calculations for the non-metallated oxaborane anion $[OB_{11}H_{12}]^-$ **2** (Fig. 5 and schematic cluster structure **II**) and the oxaferraborane $[(\eta^6\text{-}(C_6H_3Me_3)\text{-}FeOB_8H_{10}]$ **5** (Fig. 6 and schematic cluster structure **V**), using the $\{Fe(\eta^6\text{-}C_6H_6)\}$ analogue $[(\eta^6\text{-}(C_6H_6)FeOB_8H_{10}]$ **5A** as a reasonable model for **5**. Of these two, compound **5**/**5A** exhibits the most closely related structural precedent to the new oxaruthenaborane **7**.

TABLE III
Measured[a] interatomic distances for $[1\text{-}(\eta^6\text{-}C_6Me_6)\text{-}nido\text{-}6\text{-}RuB_9H_{13}]$ **8** and calculated distances for $[1\text{-}(\eta^6\text{-}C_6H_6)\text{-}nido\text{-}6\text{-}RuB_9H_{13}]$ **8A**, together with the calculated distances for $[(\eta^6\text{-}C_6Me_6)RuOB_9H_{13}]$ **7** (in Å)

Atoms	Compound **7**	Compound **8**	
	calculated	calculated	measured
Ru(1)–B(3)	2.226	2.197	2.181(9)
Ru(1)–B(2)	2.297	2.252	2.220(9)
Ru(1)–B(4)	2.294	2.250	2.214(7)
Ru(1)–B(5)	2.390	2.111	2.086(7)
Ru(1)–B(10)	2.390	2.111	2.084(8)
B(5)–B(10)	2.656	2.672	2.497(8)
B(7)–B(8)	1.828	1.804	1.835(13)
B(5)–B(6)	1.806	1.742	1.745(11)
B(9)–B(10)	1.805	1.739	1.717(12)
B(2)–B(6)	1.749	1.748	1.735(12)
B(4)–B(9)	1.749	1.745	1.721(12)
B(6)–B(7)	1.848	1.846	1.823(14)
B(8)–B(9)	1.803	1.845	1.793(14)
B(5)–H(5,6)	1.600	1.390	1.13(4)
B(6)–H(5,6)	1.240	1.307	1.25(3)
B(7)–H(6,7)	1.323	1.312	1.22(3)
B(6)–H(6,7)	1.322	1.326	1.11(3)

[a] Measured data taken from lit.[11]; $CDCl_3$, 294–300 K.

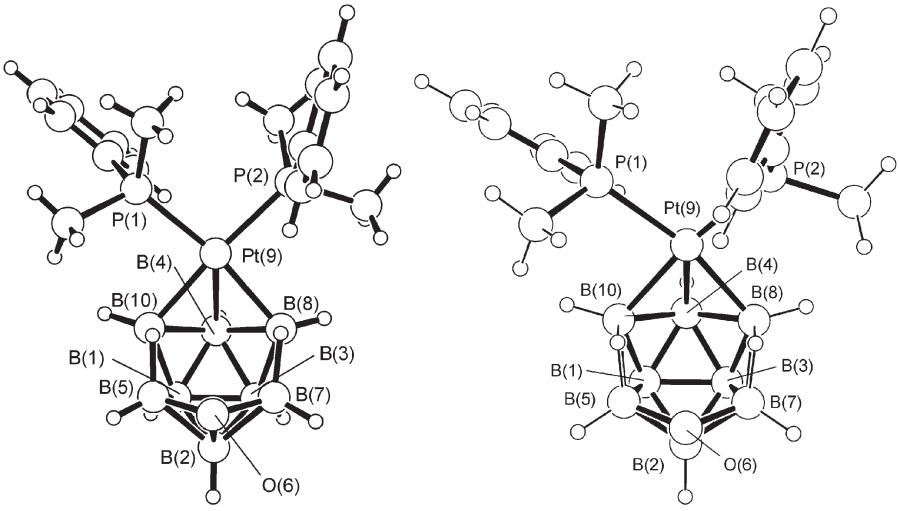

FIG. 4

The crystallographically determined[10] molecular structure of [9,9-$(PMe_2Ph)_2$-*arachno*-9,6-$PtOB_8H_{10}$] **6** (left-hand diagram) and its calculated molecular structure **6A** (DFT; B3LYP/6-31G*) (right-hand diagram). Selected interatomic distances, ordered as measured [calculated], are as follows: Pt(9)–P(1) 2.299(2) [2.395], Pt(9)–P(2) 2.300(2) [2.377], Pt(9)–B(4) 2.198(7) [2.237], Pt(9)–B(10) 2.232(7) [2.254], Pt(9)–B(8) 2.236(7) [2.250], B(5)–B(10) 1.84(1) [1.850], B(7)–B(8) 1.84(1) [1.853], B(7)–O(6) 1.508(9) [1.508], O(6)–B(5) 1.504(9) [1.506] and O(6)–B(2) 1.559(8) [1.553] Å. Boron magnetic nuclear shieldings, as calculated by GIAO techniques, and expressed as $\delta(^{11}B)$ values, are as follows: B(8,10) –15.7, B(1,3) –26.5; B(5,7) –0.5, B(4) +35.1 and B(2) +6.6 ppm; the corresponding measured values[10] are: B(8,10) –22.6, B(1,3) –26.5; B(5,7) +0.4, B(4) +33.9 and B(2) +5.1 ppm

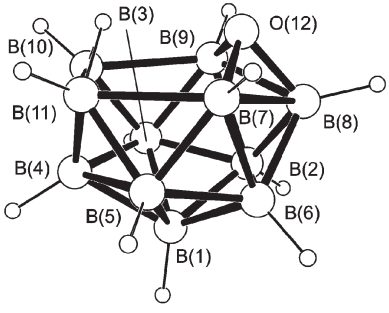

FIG. 5

Calculated molecular structure (DFT; B3LYP/6-31G*) for the $[OB_{11}H_{12}]^-$ anion **2**. Selected interatomic distances are as follows: O(12)–B(7) 1.497, O(12)–B(8) 1.465 and O(12)–B(9) 1.497; B(8)–B(7) 1.939, B(8)–B(9) 1.940, B(8)–B(2) 1.760, B(10)–B(11) 1.798 and B(7)–B(11) 2.027 Å

The structure of the anionic species **2** has not been determined crystallographically, although its structure had been calculated at the AM-1 level for thermodynamic stability comparisons[5]. No corresponding calculations of boron nuclear shieldings have previously been reported, so in a limited sense the structure is hitherto not rigorously confirmed. However, the present DFT/GIAO calculations for **2** now give ^{11}B nuclear shieldings that do closely match those obtained experimentally (Table IV), thereby giving additional support for this structure, as well as the additional confidence in the applicability of these types of calculations for polyhedral oxaborane species in general.

In contrast to anion **2**, the molecular structure of the oxaferraborane **5** has been determined experimentally, and, again, our calculated structural results for the model species $[(\eta^6\text{-}(C_6H_6)FeOB_8H_{10}]$ **5A** closely mimic those obtained experimentally for $[(\eta^6\text{-}(C_6H_3Me_3)FeOB_8H_{10}]$ **5** (Fig. 6). There are no significant discrepancies around the metal atom, in contrast to our findings for the platinum species **6**. However, for **5**, no experimentally determined boron nuclear shieldings are available, presumably because the trace quantities of **5** that were obtained experimentally were too small to permit

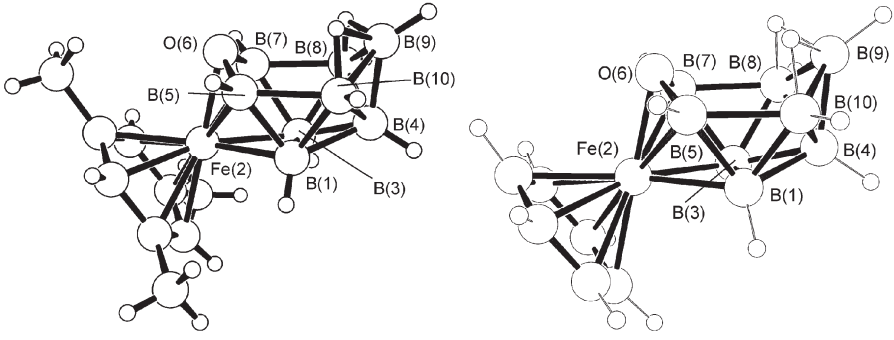

FIG. 6

Drawings of the crystallographically determined molecular structure for $[(\eta^6\text{-}C_6H_3Me_3)\text{-}FeOB_8H_{10}]$ **5** (left-hand diagram)[9]; and the calculated molecular structure (DFT; B3LYP/6-31G*) for the $[(\eta^6\text{-}C_6H_6)FeOB_8H_{10}]$ model compound **5A** (right-hand diagram). Selected interatomic distances, ordered as measured for **5** [calculated for **5A**], are as follows: Fe(2)–B(1) 2.086(6) [2.121], Fe(2)–B(3) 2.072(8) [2.120], Fe(2)–B(5) 2.054(6) [2.076], Fe(2)–O(6) 1.942(3) [1.965], Fe(2)–B(7) 2.053 (7) [2.073], O(6)–B(5) 1.423(7) [1.444], O(6)–B(7) 1.428(8) [1.445] and B(5)–B(10) 1.91(1) [1.930] Å. Interestingly, the calculated interatomic distances seem to be predominantly at the outer edge of the standard uncertainties (3σ) for the measured values. Boron magnetic nuclear shieldings, as calculated by GIAO techniques, and expressed as $\delta(^{11}B)$ values, are as follows: B(5,7) +13.27, B(1,3) +13.31; B(9) +10.39, B(8,10) –3.38 and B(4) –36.49 ppm

TABLE IV
Measured[a] and calculated NMR chemical shifts δ(^{11}B) for the $[OB_{11}H_{12}]^-$ anion **2**

Position	Calculated	Measured	Difference
B(1)	+11.52	+11.3	+0.2
B(10,11)	+11.02	+12.8	–1.8
B(8)	+2.87	+4.3	–1.4
B(7,9)	–6.48	–7.0	+0.5
B(2,5)	–15.36	–14.1	–1.3
B(3,4)	–17.07	–16.4	–0.7
B(6)	–29.20	–29.1	–0.1

[a] Measured data taken from lit.[2,4]; $CDCl_3$, 294–300 K.

NMR measurements with instrumentation then available[9]. Nevertheless our calculated boron nuclear shielding values (see caption to Fig. 6) may be of use for future correlation and comparison work.

In sum, the formulation and the structure of the oxaruthenaborane $[(\eta^6\text{-}C_6Me_6)RuOB_9H_{13}]$ **7** are both reasonably substantiated. In terms of isolobal analogy, if the {Ru(η^6-C_6Me_6)} vertex is regarded as a {BH} vertex-mimic[13], and the {O} vertex as a $\{BH_2\}^-$ mimic that contributes two orbitals and two electrons to the cluster bonding proper[9,13], then compound **7** is an eleven-vertex [*arachno*-$B_{11}H_{16}]^-$ cluster-equivalent. Consistent with this, an *arachno* descriptor for the eleven-vertex $\{MOB_9\}$ skeleton of **7** (schematic **VII C**) would be in accord with the Williams/Wade structure-geometry/cluster-electron-count paradigm[13–16] in that it is generated by the removal of two adjacent vertices from the *closo* thirteen-vertex 1:6:5:1 stack (schematic **XI**).

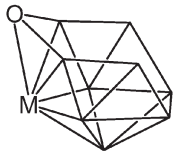

VII C

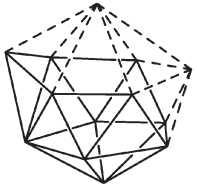

XI

The substantiation of another of these rare and sporadically encountered, but nevertheless quite stable, contiguous oxaborane species may be of some portent, in that it suggests that reasonably extensive larger oxaborane families are potentially stable and isolatable. In this regard it may be noted that

the cluster incorporation of sulfur, the closest Group-16 congener of oxygen, engenders extensive borane-cluster flexibility, and sulphur is consequently a component of an increasingly large and versatile series of thiaboranes and thiametallaboranes[17–20]. Stoichiometric reactions with potential oxygen-atom sources such as hydroxides, oxides, peroxides and superoxides may constitute suitable entries to designed oxaborane syntheses. Here the requirement for an exact reagent stoichiometry may well be critical: essentially universally in previously reported reactions of polyhedral boron-containing cluster compounds with such oxygen-containing reagents, these reagents have been used in excess, rather than stoichiometrically, generally resulting in general nucleophilic or oxidative cluster dismantlings, ultimately to give mononuclear oxyborates, and thence inherently precluding the incorporation of single oxygen atoms into the cluster.

The mechanism of formation of the oxametallaborane species **8** is at present necessarily obscure, particularly in view of the very low yield and the large variety of other products in the reaction product mixture from which **8** was isolatable (see below). In this context, however, it may be noted that there is a recent report of a well-defined and stoichiometric uptake of dioxygen at a metallaborane metal site, specifically by twelve-vertex $[(PMe_2Ph)_4Pt_2B_{10}H_{10}]$ **10** [21]. This occurs very readily, and readily reversibly, to give the peroxidic dioxygen–dimetallaborane complex $[(PMe_2Ph)_4(O_2)Pt_2B_{10}H_{10}]$ **11**. However, the structure of the last compound **11** is quite different to that of $[(\eta^6\text{-}C_6Me_6)RuOB_9H_{13}]$ (species **7**): it exhibits an *exo*-cluster peroxide-like dioxygen bridge across two mutually bonded metal atoms, rather than oxygen assimilation by the cluster to give a contiguous oxametallaborane cluster assembly as in the schematics **I**–**VII** above. On the other hand, the initial dioxygen adduct **11** readily decomposes at room temperature in solution to give as yet uncharacterised platinaborane species that may contain oxygen atoms incorporated into their cluster matrices[21,22]. It will be of interest to elucidate these species.

In summary, although contiguous oxaborane cluster species are few in number, the stability of those that are known portend a more extensive oxaborane and oxametallaborane chemistry. In this context it is noted that the thiaborane and thiametallaborane chemistry of sulfur, the closest Group IV congener of oxygen, is increasingly recognised for its variety and flexibility[23].

Incidental to the novelty of the oxaruthenaborane **7** and its implications, to complete this report it is apposite to include a brief listing of the other

products of the reaction between the *arachno* six-vertex $[B_6H_{11}]^-$ anion and $[\{RuCl_2(\eta^6\text{-}C_6Me_6)\}_2]$ that yields compounds **7**, **8** and **9**. Preliminary reports of some aspects have been published previously[11,24]. Initially, deprotonation of *nido*-B_5H_9 to give the $[nido\text{-}B_5H_8]^-$ anion was effected by the use of KH in THF solution at low temperature, and thence the addition of B_2H_6 gave the $[arachno\text{-}B_6H_{11}]^-$ anion[25]. Addition of CH_2Cl_2 and thence $[\{RuCl_2(\eta^6\text{-}C_6Me_6)\}_2]$, still at low temperature, followed by warming to, and further reaction at, room temperature gave a mixture of many products, of which most were in low yield, some very low. Chromatographic separation thence resulted in the isolation of compounds **7** (0.2%), **8** (ca. 9%) and **9** (ca. 5%), as just mentioned above, together with three previously described[23,26,27] species $[2\text{-}(\eta^6\text{-}C_6Me_6)\text{-}2\text{-}Cl\text{-}arachno\text{-}RuB_3H_8]$ **12** (schematic cluster structure **XII**)[26] (occasional incidence in low yield), $[2\text{-}(\eta^6\text{-}C_6Me_6)\text{-}n\text{-}arachno\text{-}2\text{-}RuB_8H_{14}]$ **13** (schematic cluster structure **XIII**)[23] (0.5%), and $[5\text{-}(\eta^6\text{-}C_6Me_6)\text{-}nido\text{-}5\text{-}RuB_9H_{13}]$ **14** (schematic cluster structure **XIV**)[27] (ca. 5%), readily identified by spectroscopic comparison with the literature data. Five other isolatable compounds were previously undescribed species. Two of these, $[2\text{-}(\eta^6\text{-}C_6Me_6)\text{-}nido\text{-}2\text{-}RuB_4H_8]$ **15** (schematic cluster structure **XV**) (ca. 1.5%) and $[4\text{-}(\eta^6\text{-}C_6Me_6)\text{-}nido\text{-}4\text{-}RuB_5H_9]$ **16** (schematic cluster structure **XVI**) (ca. 5.5%), were variants on well-known species[28–30], and were readily characterised by spectroscopic comparison (see Experimental). Three other new species were present in sub-milligram quantities only (<0.1%). The very small quantities permitted only provisional characterisation, but nevertheless we present the results here. Two of the three were tentatively identified as the *commo*-2-Ru-bi(*nido*-six-vertex) species $[H_{10}B_5RuB_5H_{10}]$ **17** (schematic cluster structure **XVII**) and as $[1\text{-}(\eta^6\text{-}C_6Me_6)\text{-}1\text{-}H\text{-}arachno\text{-}1\text{-}RuB_4H_9]$ **18** (schematic cluster structure **XVIII**); again these two were simple variants on reported species[31–37], allowing their identification by spectroscopic comparison (see Experimental). The remaining compound is proposed to be $[4\text{-}(\eta^6\text{-}C_6Me_6)\text{-}n\text{-}arachno\text{-}4\text{-}RuB_8H_{14}]$ **19** of previously unreported nine-vertex metallaborane configuration **XIX**, isomeric with the previously reported[23] compound $[2\text{-}(\eta^6\text{-}C_6Me_6)\text{-}n\text{-}arachno\text{-}2\text{-}RuB_8H_{14}]$ **13** (schematic cluster structure **XIII**) mentioned above. The empirical formula of **19** is consistent with the results of multinuclear NMR spectroscopy and mass spectrometry, and the ^{11}B nuclear shieldings as calculated for the DFT-minimised molecular structure of the $[4\text{-}(\eta^6\text{-}C_6H_6)\text{-}n\text{-}arachno\text{-}4\text{-}RuB_8H_{14}]$ analogue **19A** (Fig. 7 (left)) reasonably match those determined experimentally (see Experimental). The exception to this generalisation is for the B(3) position, which is in an exposed $\{BH_2\}$ grouping adjacent to the Ru(4) centre, and which has a discrepancy between observed and calculated ^{11}B nuclear magnetic shieldings of

8.3 ppm. Elements of this discrepancy may arise because of steric or electronic affects associated with the adjacent C_6Me_6 ligand in **19** versus the C_6H_6 ligand in **19A**. In any event, all the other shieldings correspond within 2.8 ppm, which is not unreasonable for a metallaborane of a second-row transition element for calculations at the B3LYP/6-31G* level of theory used, and the experimentally observed ^{11}B shielding values are fundamentally different from those calculated for the only other isomeric possibility, the [5-(η^6-C_6H_6)-*n-arachno*-5-RuB_8H_{14}] isomer **20** (Fig. 7 (right)).

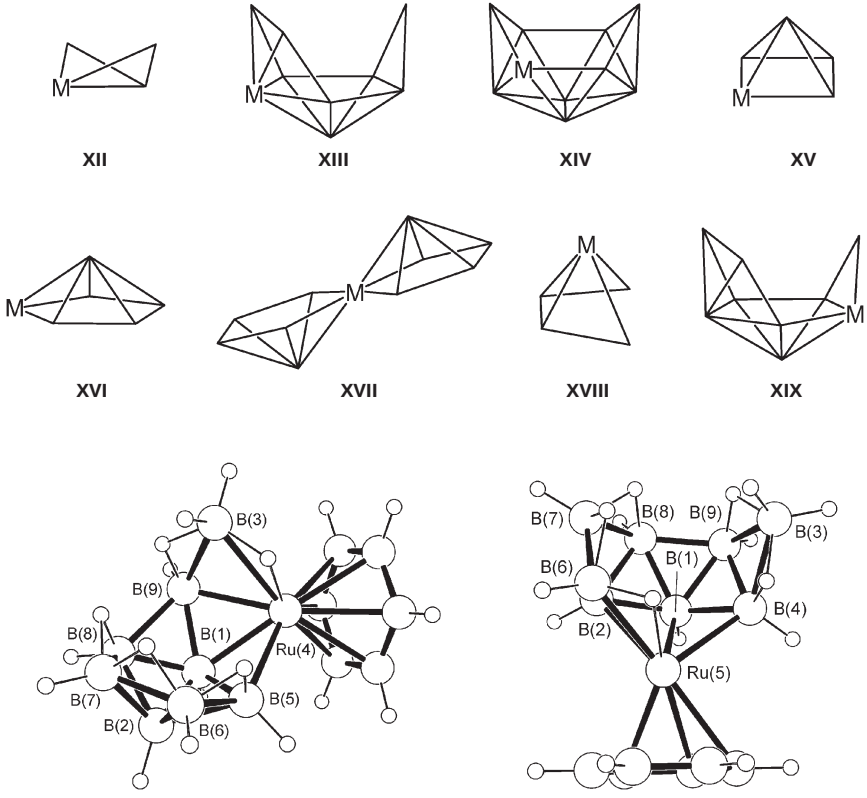

FIG. 7

Drawings of molecular structures calculated using DFT at the B3LYP/6-31G* level. The left-hand diagram is for the [4-(η^6-C_6H_6)-*n-arachno*-4-RuB_8H_{14}] model compound **19A**. The calculated ^{11}B nuclear shieldings for this structure closely match those observed experimentally for compound **19** of proposed formulation [4-(η^6-C_6Me_6)-*n-arachno*-4-RuB_8H_{14}] (see Experimental), which in turn do not correspond to those calculated for the [5-(η^6-C_6H_6)-*n-arachno*-5-RuB_8H_{14}] model **20A** (right-hand diagram) of the only other isomeric possibility [5-(η^6-C_6Me_6)-*n-arachno*-5-RuB_8H_{14}] **20**

These yields for the fourteen compounds **7–20** given here are typical, although it is emphasised that, in our hands, the ratio of the products varied considerably from reaction to reaction, even when carried out under ostensibly identical conditions: for example, the incidence of compound **16** varied from 5–26%. This may be due to subtle variations in the exact provenance of the starting materials used, a phenomenon often noted in reactions that give several low-yield metallaborane products[38]. However, in the present case the number of major products isolated was essentially invariant.

EXPERIMENTAL

General

Preparative thin-layer chromatography (TLC) was carried out using 1 mm layers of silica gel G (Merck, type GF254), made from water slurries on glass plates of dimensions 20 × 20 cm, followed by drying in air at 80 °C. Eluted TLC components were extracted from the silica matrix with CH_2Cl_2, and evaporated to dryness for further examination and/or manipulation. HPLC was performed on a 16 mm × 25 cm column (Knauer, Lichosorb Si60, 7 mm) using a flow rate of 10 ml min^{-1}, with detection by change in the UV absorption of the eluate, as monitored at λ 254 nm. NMR spectroscopy was performed at ca. 2.3 and 9.4 T (fields respectively corresponding to nominal 100 and 400 MHz ^1H frequencies) using commercially available instrumentation and using techniques and procedures as adequately described and enunciated elsewhere[39–44]. Spectra were recorded at 294–297 K for solutions in $CDCl_3$. Chemical shifts δ are given in ppm relative to Ξ = 100 MHz for δ(^1H) (±0.05 ppm) (nominally TMS) and Ξ = 32.083972 MHz for δ(^{11}B) (±0.5 ppm) (nominally Et_2OBF_3 in $CDCl_3$)[29]. Ξ is as defined by McFarlane[45]. Cluster ^{11}B and ^1H NMR data are presented in the order: assignment δ(^{11}B) (δ(^1H) of directly bound terminal hydrogen atom in square brackets). Mass spectrometric data are from positive-ion 70 eV electron-ionisation spectra. As mentioned in the discussion above, the yields of the metallaboranes varied among repeated experiments; the following describes typical results from the sequence of reaction and isolation.

Reaction of the [*arachno*-$B_6H_{11}]^-$ Anion with [{$RuCl_2(\eta^6$-$C_6Me_6)$}$_2$]

The [*arachno*-$B_6H_{11}]^-$ anion was initially made in situ essentially according to the procedure of Johnson, Geanangel and Shore[25]. Thus, using standard vacuum-line technique, B_5H_9 (17.9 mmol) and THF (100 ml) were condensed onto KH (70% active, 1.02 g, corresponding to 17.9 mmol KH) in a reaction vessel equipped with a magnetic stirrer-bar and a tipper-tube containing [{$RuCl_2(\eta^6$-$C_6Me_6)$}$_2$] (800 mg, 1.2 mmol). The reaction mixture was stirred at –78 °C for 1 h to give a solution of the K^+ salt of the [*nido*-$B_5H_8]^-$ anion. B_2H_6 (8.9 mmol) was then condensed into the reaction mixture at –78 °C and the mixture then stirred at –78 °C for 40 min to give a solution of the K^+ salt of the [*nido*-$B_6H_{11}]^-$ anion. The [{$RuCl_2(\eta^6$-$C_6Me_6)$}$_2$] was then added from the tipper-tube, and the mixture was then warmed to –25 °C and stirred at –25 °C for 2 h. It was then warmed to room temperature, and exposed to air. Subsequent manipulations were carried out in air. The mixture was filtered through silica, first

with the aid of CH_2Cl_2, and then with MeCN. The CH_2Cl_2 extract was evaporated to dryness, and the residue redissolved in CH_2Cl_2 (ca. 5 ml) and applied to preparative TLC plates, which were then developed using CH_2Cl_2/hexane (50:50) as the liquid phase. This gave four major components: **A**, colourless (detected under UV illumination), R_F ca. 0.8, identified by NMR spectroscopy as *nido*-$B_{10}H_{14}$; **B**, yellow, R_F around 0.65, a complex mixture, which overlapped with **C**, yellow, R_F ca. 0.6, identified by NMR spectroscopy as the previously described species [5-(η^6-C_6Me_6)-*nido*-5-RuB_9H_{13}] **14** [27] (46 mg, 5.1%), and **D**, yellow, R_F ca. 0.5, identified as [4-(η^6-C_6Me_6)-*nido*-4-RuB_5H_9] **16** (41 mg, 5.3%) as described below. An occasional trace product **E**, yellow, R_F ca. 0.1, was identified by NMR spectroscopy as the previously described species [2-(η^6-C_6Me_6)-2-Cl-*arachno*-RuB_3H_8] **12** [26]. NMR spectroscopy showed that the boron-containing components of the MeCN extract were principally the [*arachno*-B_3H_8]$^-$ and [*arachno*-B_9H_{14}]$^-$ anions, presumably with K^+ as counter-cation.

The complex mixture **B** was then separated by HPLC, using CH_2Cl_2/hexane (30:70) as liquid phase, to give eight yellow components: **F**, R_T ca. 5 min, tentatively characterised as the *commo*-2-Ru-bi(*nido* six-vertex) species [$H_{10}B_5RuB_5H_{10}$] **17** by the data described below (<1 mg, trace quantity); **G**, R_T ca. 7 min, tentatively characterised as [4-(η^6-C_6Me_6)-*n-arachno*-4-RuB_8H_{14}] **19** by the data described below (<1 mg, trace quantity); **H**, R_T ca. 7.5 min, identified by NMR spectroscopy as the previously described species [2-(η^6-C_6Me_6)-*nido*-2-RuB_9H_{13}] **9** [11] (42 mg, 4.7%); **I**, R_T ca. 11.5 min, identified by NMR spectroscopy as the previously described species [1-(η^6-C_6Me_6)-*nido*-1-RuB_9H_{13}] **8** [11] (42 mg, 4.7%); **J**, R_T ca. 12 min, identified by NMR spectroscopy as the previously described species [2-(η^6-C_6Me_6)-*n-arachno*-2-RuB_8H_{14}] **13** [23] (4 mg, 0.5%); **K**, R_T ca. 14 min, characterised as [2-(η^6-C_6Me_6)-*nido*-2-RuB_4H_8] **15** as described below (11 mg, 1.5%); **L**, R_T ca. 14.5 min, characterised as [1-(η^6-C_6Me_6)-1-H-*arachno*-1-RuB_4H_9] **18** as described below (<1 mg, trace quantity); and **M**, R_T ca. 19 min, characterised as [(η^6-C_6Me_6)$RuOB_9H_{13}$] **7** as described above in the main body of the text (2 mg, 0.2%).

Characterisation Data for New Species **15** and **16**

[2-(η^6-C_6Me_6)-nido-2-RuB_4H_8] **15**. NMR data, presented as $\delta(^{11}B)$ ($\delta(^1H)$ of directly bound exo hydrogen atom in square brackets): BH(4) +2.9 [–3.86], BH(2,5) –12.2 [+1.84] and BH(1) –18.4 [+1.01], with $\delta(^1H)$ for μH(2,3)(2,5) –11.43, μH(3,4)(4,5) –2.93 and {C_6Me_6} +2.25; compare reported data for other known *nido*-2-metallapentaboranes such as [2-(η^5-C_5H_5)-*nido*-2-CoB_4H_8] and related species[28,29]. The mass spectrum exhibited a highest *m/z* cut-off corresponding to the highest isotopomer of the molecular ion M^+. For {$C_{12}H_{26}B_4Ru$} calculated: 45.8% C, 8.3% H, 11.6% B; found: 47.6% C, 8.4% H, 10.6% B.

[4-(η^6-C_6Me_6)-nido-4-RuB_5H_9] **16**. NMR data, presented as $\delta(^{11}B)$ ($\delta(^1H)$ of directly bound exo hydrogen atom in square brackets): BH(1) –17.7 [–1.04], BH(2,6) +20.2 [+4.41] and BH(3,5) +40.1 [+5.59], with $\delta(^1H)$ for μH(2,3)(5,6) –2.89, μH(2,3)(5,6) –2.89 and {C_6Me_6} +2.28; compare reported data for [4,4,4-(CO)$(PPh_3)_2$-*nido*-4-RuB_5H_9] [30]. The mass spectrum exhibited a highest *m/z* cut-off corresponding to the highest isotopomer of the molecular ion M^+. For {$C_{12}H_{27}B_5Ru$} calculated: 44.1% C, 8.2% H; found: 43.0% C, 8.2% H. Additionally, a single-crystal X-ray diffraction study of the molecule is reported elsewhere in a more general structural context[46].

Characterisation Data for New Species **17**, **18** and **19**

These three very low-yield product species, tentatively formulated as the *commo*-2-Rubi(*nido*-six-vertex) species $[H_{10}B_5RuB_5H_{10}]$ **17**, as $[1\text{-}(\eta^6\text{-}C_6Me_6)\text{-}1\text{-}H\text{-}arachno\text{-}1\text{-}RuB_4H_9]$ **18**, and as $[4\text{-}(\eta^6\text{-}C_6Me_6)\text{-}n\text{-}arachno\text{-}4\text{-}RuB_8H_{14}]$ **19**, were only obtainable in sub-milligram quantities in the pure state. The tentative formulations of **17** and **18** are based principally on comparison of NMR parameters with known structural analogues. Compound **19**, with no direct structural analogue, is formulated on the basis of DFT calculations of structure (Fig. 7) and thence calculated ^{11}B nuclear shieldings that match those observed experimentally.

$[H_{10}B_5RuB_5H_{10}]$ **17**. NMR data only: the iron analogue $[H_{10}B_5FeB_5H_{10}]$ is known[31], and the NMR spectra may be assigned on the basis of the reported spectra for $[H_6C_6FeB_5H_{10}]$ and related cobalt and manganese congeners[32–34]. Cluster NMR data are presented in the order: assignment $\delta(^{11}B)$ ($\delta(^1H)$ of directly bound terminal hydrogen atom in square brackets): BH(1) –49.0 [–0.49], BH(4,5) +10.1 [+4.10] and BH(3,6) +36.9 [+6.26], with $\delta(^1H)$ for μH(2,3)(2,6) –12.79, μH(3,4)(5,6) +0.02 and μH(4,5) –1.13; no signal for any C_6Me_6 protons was present.

$[1\text{-}(\eta^6\text{-}C_6Me_6)\text{-}1\text{-}H\text{-}arachno\text{-}1\text{-}RuB_4H_9]$ **18**. Cluster NMR data are presented in the order: assignment $\delta(^{11}B)$ ($\delta(^1H)$ of directly bound terminal hydrogen atom in square brackets): BH(2,5) –8.4 [+1.60 (2 H), +1.98 (2 H)] and BH(3,4) +0.2 [+1.99 (2 H)], with $\delta(^1H)$ for μH(3,4) –3.92, μH(2,3)(4,5) –4.40, $\{C_6Me_6\}$ +2.20 and RuH –11.17 (apparent 1:2:1 triplet, repeated splitting ca. 10 Hz from inter-proton couplings; also some unresolved coupling to $^{11}B(2,5)$); compare reported data for $[1,1,1,1\text{-}(CO)(PMe_3)_2H\text{-}arachno\text{-}1\text{-}IrB_4H_9]$[35,36] and for *arachno*-B_5H_{11} itself[37]. The mass spectrum exhibited a highest *m/z* cut-off value corresponding to the highest isotopomer of the molecular ion M^+; the highest-mass envelope also contained significant contributions from $(M - 1)^+$ and $(M - 2)^+$ ions, indicating ready hydrogen loss.

$[4\text{-}(\eta^6\text{-}C_6Me_6)\text{-}n\text{-}arachno\text{-}4\text{-}RuB_8H_{14}]$ **19**. NMR data only; cluster NMR data are presented in the order: assignment $\delta(^{11}B)$(observed) ($\delta(^{11}B)$(calculated for $[4\text{-}(\eta^6\text{-}C_6H_6)\text{-}n\text{-}arachno\text{-}4\text{-}RuB_8H_{14}]$ **19A** at the B3LYP-631G* level in braces) ($\delta(^1H)$ of directly bound terminal hydrogen atom in square brackets): BH(1) +13.9 {+11.1} [+3.06], BH(2) –49.0 {–51.1} [–0.52], BH(3) –6.8 {–15.2} [+1.71 (*exo*) and +0.31 (*endo*)], BH(5) +1.9 {+3.5} [+2.54], BH(6) +0.6 {–0.9} [+3.23], BH(7) +9.0 {+6.5} [+3.63], BH(8) +6.4 {+7.4} [+3.41] and BH(9) –6.8 {–5.0} [+2.18], with $\delta(^1H)$ for $\{C_6Me_6\}$ +2.15, μH(3,4) –13.30; also (assignments tentative) μH(5,6) and μH(6,7) –2.70 and –1.45, μH(7,8) –2.14 and μH(3,9) –3.85. Seven $[^{11}B\text{-}^{11}B]$-COSY correlations were observed as follows: B(1)–B(2) w, B(1)–B(5) s, B(1)–B(8) m, B(1)–B(9) s, B(2)–B(7) w, B(2)–B(8) m and B(2)–B(6) s. The possibility that this may be the 5-isomer, viz. $[5\text{-}(\eta^6\text{-}C_6Me_6)\text{-}n\text{-}arachno\text{-}5\text{-}RuB_8H_{14}]$ **20**, is discounted on the basis that the ^{11}B shieldings, as calculated for the DFT-calculated energetically minimum molecular structure of the $\{Ru(C_6H_6)\}$ analogue $[5\text{-}(\eta^6\text{-}C_6H_6)\text{-}n\text{-}arachno\text{-}5\text{-}RuB_8H_{14}]$ **20A** (Fig. 7 (right)) are at considerable general variance to those observed experimentally, taking the following $\delta(^{11}B)$ values: B(1) +24.8, B(2) –26.3, B(3) –6.7, B(4) –26.0, B(6) +20.9, B(7) +6.0, B(8) –9.9 and B (9) –35.7.

Structural and Shielding Calculations

For the density-functional theory (DFT) calculations structures were initially optimised with the STO-3G* basis set for B, C, P, H and O and with the LANL2DZ basis set for the metal atom in the metallaboranes, using standard ab initio methods as incorporated in the Gaussian-98 package[47]. The final optimisations, including frequency analyses to confirm the true minima, together with GIAO NMR nuclear-shielding predictions, were performed using

B3LYP methodology, again with the 6-31G* basis set for B, C, P, O and H, but now with the LANL2DZ basis set for the metal atom. For compound **7**, a structure to represent [1-(η^6-C_6Me_6)-*nido*-1-RuB_9H_{13}] was initially optimised starting from the {Ru(η^6-C_6H_6)} analogue **7A** of compound **7**, with an approximate geometry as represented in schematic **VII** that was derived by the positioning of an oxygen atom on the crystallographically established[11] structural co-ordinates of [1-(η^6-C_6Me_6)-*nido*-1-RuB_9H_{13}] **8** (Fig. 1). The final optimisation for compound **7** thence started from this initially optimised geometry for **7A**, but now with the incorporation of six methyl groups to give a {Ru(η^6-C_6Me_6)} unit rather than {Ru(η^6-C_6H_6)}. The energetic minimum is represented in Fig. 3 as a molecular structure, and the boron nuclear shieldings, expressed as $\delta(^{11}B)$ values, are summarised and compared with the experimentally measured values in Table I. Similar procedures were used for the calculations on the other compounds. Drawings of molecular structures were made using the ORTEP-3 program[48].

SUPPLEMENTARY DATA

Calculated atomic coordinates (DFT; B3LYP/6-31G*) for the $[OB_{11}H_{12}]^-$ anion **2** and (DFT; B3LYP/6-31G*, LANL2DZ) for [(η^6-C_6H_6)$FeOB_8H_{10}$] **5A**, [$(PMe_2Ph)_2PtOB_8H_{10}$] **6**, [(η^6-C_6Me_6)-$RuOB_9H_{13}$] **7**, [(η^6-C_6H_6)RuB_9H_{13}] **8A** and [4-(η^6-C_6H_6)-*n-arachno*-4-RuB_8H_{14}] **19A**. These are available on http://cccc/uochb.cas.cz/Vol/70/No04/20050410.html.

We thank the UK SERC (now superseded by the UK EPSRC) for a studentship to M. Bown, and for previous equipment grants. Recent aspects of the work have been supported by personal financial and computing equipment contributions from J. Bould, and some earlier aspects by personal financial contributions from D. Kennedy, whom we thank.

REFERENCES

1. Jelínek T., Kennedy J. D., Štíbr B., Thornton-Pett M.: *J. Chem. Soc., Chem. Commun.* **1995**, 1665.
2. Ouassas A., R'Kha C., Mongeot H., Frange B.: *Inorg. Chim. Acta* **1991**, *180*, 257.
3. Ouassas A., Fenet B., Mongeot H., Frange B. in: *Current Topics in the Chemistry of Boron* (G. Kabalka, Ed.), p. 363. The Royal Society of Chemistry, Cambridge 1994.
4. Ouassas A., Fenet B., Mongeot H., Frange B., Gautheron B., Barday E.: *J. Chem. Soc., Chem. Commun.* **1995**, 1663.
5. Serrar C., Ouassas A., Boutalib A., Barday E., Gautheron B., Hanquet B., Frange B.: *Main Group Met. Chem.* **1997**, *20*, 247.
6. Frange B., Kennedy J. D.: *Main Group Met. Chem.* **1996**, *19*, 175.
7. Fontaine X. L. R., Fowkes H., Greenwood N. N., Kennedy J. D., Thornton-Pett M.: *J. Chem. Soc., Chem. Commun.* **1985**, 1722.
8. Ditzel E. J., Fontaine X. L. R., Fowkes H., Greenwood N. N., Kennedy J. D., MacKinnon P., Sisan Z., Thornton-Pett M.: *J. Chem. Soc., Chem. Commun.* **1990**, 1692.
9. Micciche R. P., Briguglio J. J., Sneddon L. G.: *Inorg. Chem.* **1984**, *23*, 3992.
10. Kim Y.-H., Greatrex R., Kennedy J. D.: *Collect. Czech. Chem. Commun.* **1997**, *62*, 1289.

11. a) Bown M., Fontaine X. L. R., Greenwood N. N., Kennedy J. D., MacKinnon P.: *J. Chem. Soc., Chem. Commun.* **1987**, 817; b) Bown M.: *PhD. Thesis*. University of Leeds, Leeds, 1987.
12. Tippe A., Hamilton W.: *Inorg. Chem.* **1969**, *8*, 464.
13. Wade K.: *Adv. Inorg. Chem. Radiochem.* **1976**, *18*, 1.
14. Williams R. E.: *Inorg. Chem.* **1971**, *10*, 210.
15. Wade K.: *J. Chem. Soc., Chem. Commun.* **1971**, 792.
16. Williams R. E.: *Adv. Inorg. Chem. Radiochem.* **1976**, *18*, 67.
17. Jelínek T., Kennedy J. D., Štíbr B., Thornton-Pett M.: *Angew. Chem., Int. Ed. Engl.* **1994**, *33*, 1599.
18. Binder H., Hein M.: *Coord. Chem. Rev.* **1997**, *158*, 171.
19. a) Todd L. J. in: *Comprehensive Organometallic Chemistry I* (E. W. Abel, G. W. Wilkinson and F. G. A. Stone, Eds), Vol. 1, Chap. 5.6, p. 543. Pergamon, Oxford 1982; b) Todd L. J., Arafat A., Baer J., Huffman J. C. in: *Advances in Boron and the Boranes* (J. F. Liebman, A. Greenberg and R. E. Williams, Eds), p. 287. VCH, Weinheim 1988.
20. Carr M. J., Londesborough M. G. S., Bould J., Císařová I., Štíbr B., Kennedy J. D.: *Collect. Czech. Chem. Commun.* **2005**, *70*, 430.
21. Bould J., McInnes Y. M., Carr M. J., Kennedy J. D.: *Chem. Commun.* **2004**, 2380.
22. Bould J., Kilner C. A., Kennedy J. D.: *Dalton Trans.* **2005**, in press.
23. a) Macías R., Holub J., Clegg W., Thornton-Pett M., Štíbr B., Kennedy J. D.: *J. Chem. Soc., Dalton Trans.* **1997**, 149; b) Jelínek T., Kennedy J. D., Štíbr B., Thornton-Pett M.: *Inorg. Chem. Commun.* **1998**, *1*, 179; c) Jelínek T., Císařová I., Štíbr B., Kennedy J. D., Thornton-Pett M.: *J. Chem. Soc., Dalton Trans.* **1998**, 2965; d) Jelínek T., Kilner C. A., Thornton-Pett M., Kennedy J. D.: *J. Chem. Soc., Chem. Commun.* **1999**, 1905; e) Dosangh P. K., Bould J., Londesborough M. G. S., Jelínek T., Thornton-Pett M., Štíbr B., Kennedy J. D.: *J. Organomet. Chem.* **2003**, *680*, 312.
24. a) Bown M., Fontaine X. L. R., Greenwood N. N., Kennedy J. D., Thornton-Pett M.: *J. Organomet. Chem.* **1986**, *315*, C1; b) Bown M., Greenwood N. N., Kennedy J. D.: *J. Organomet. Chem.* **1986**, *309*, C67.
25. Johnson H. D., Geanangel R. A., Shore S. G.: *Inorg. Chem.* **1970**, *9*, 908.
26. Bown M., Fontaine X. L. R., Greenwood N. N., Kennedy J. D., MacKinnon P., Thornton-Pett M.: *J. Chem. Soc., Dalton Trans.* **1987**, 2781.
27. Bown M., Fontaine X. L. R., Fowkes H., Greenwood N. N., Kennedy J. D., MacKinnon P., Nestor K.: *J. Chem. Soc., Dalton Trans.* **1988**, 2597.
28. Sneddon L. G., Voet D.: *J. Chem. Soc., Chem. Commun.* **1976**, 118.
29. a) Miller V. R., Weiss R., Grimes R. N.: *J. Am. Chem. Soc.* **1977**, *99*, 5646; b) Weiss R., Bowser J. R., Grimes R. N.: *Inorg. Chem.* **1978**, *17*, 1522.
30. Greenwood N. N., Kennedy J. D., Thornton-Pett M., Woollins J. D.: *J. Chem. Soc., Dalton Trans.* **1985**, 2397.
31. Shore S. G., Ragaini J., Schmitkons T., Barton L., Medford G., Plotkin J.: *Fourth International Meeting on Boron Chemistry, IMEBORON IV, Snowbird, Utah, U.S.A., July 8–13, 1979*, Abstract No. CA07, p. 36, 1979.
32. a) Weiss R., Grimes R. N.: *J. Am. Chem. Soc.* **1977**, *99*, 8087; b) Weiss R., Grimes R. N.: *Inorg. Chem.* **1979**, *18*, 3291.
33. Borodinsky L., Grimes R. N.: *Inorg. Chem.* **1982**, *21*, 1921.
34. Fischer M. B., Gaines D. F.: *Inorg. Chem.* **1979**, *18*, 3200.
35. Bould J., Greenwood N. N., Kennedy J. D.: *J. Chem. Soc., Dalton Trans.* **1982**, 481.

36. Boocock S. K., Toft M. A., Inkrott K. E., Hsu L.-Y., Huffman J. C., Folting K., Shore S. G.: *Inorg. Chem.* **1984**, *23*, 3084.
37. a) Williams R. E., Gerhart F. J., Pier E.: *Inorg. Chem.* **1965**, *4*, 1239; b) Eaton G. R., Lipscomb W. N.: *NMR Studies of Boron Hydrides and Related Compounds*, p. 121. W. A. Benjamin, Inc., New York 1969.
38. a) Kennedy J. D.: *Prog. Inorg. Chem.* **1984**, *32*, 519; b) Kennedy J. D.: *Prog. Inorg. Chem.* **1986**, *34*, 211; more recently see also, for example: c) Bould J., Kennedy J. D., Thornton-Pett M.: *J. Chem. Soc., Dalton Trans.* **1992**, 563.
39. Kennedy J. D. in: *Multinuclear NMR* (J. Mason, Ed.), Chap. 8, p. 221. Plenum, New York and London 1987; and references therein.
40. See, for example, together with references therein: a) Heřmánek S.: *Inorg. Chim. Acta* **1999**, *289*, 20; b) Heřmánek S.: *Chem. Rev.* **1992**, *92*, 325; c) Reed D.: *Chem. Soc. Rev.* **1993**, *22*, 109.
41. Kennedy J. D., Staves J.: *Z. Naturforsch., B* **1979**, *34*, 808.
42. a) Venable T. L., Hutton W. C., Grimes R. N.: *J. Am. Chem. Soc.* **1982**, *104*, 4716; b) Venable T. L., Hutton W. C., Grimes R. N.: *J. Am. Chem. Soc.* **1984**, *106*, 29.
43. a) Fontaine X. L. R., Kennedy J. D.: *J. Chem. Soc., Chem. Commun.* **1986**, 779; b) Fontaine X. L. R., Kennedy J. D.: *J. Chem. Soc., Dalton Trans.* **1987**, 1573.
44. See, for example, together with references therein: a) Beckett M. A., Bown M., Fontaine X. L. R., Greenwood N. N., Kennedy J. D., Thornton-Pett M.: *J. Chem. Soc., Dalton Trans.* **1988**, 1969; b) Ferguson G., Kennedy J. D., Fontaine X. L. R., Faridoon, Spalding T. R.: *J. Chem. Soc., Dalton Trans.* **1988**, 2555.
45. McFarlane W.: *Proc. R. Soc. London, Ser. A* **1968**, *306*, 185.
46. Bould J., Bown M., Coldicott R. J., Ditzel E. J., Greenwood N. N., Macpherson I., MacKinnon P., Thornton-Pett M., Kennedy J. D.: *J. Organomet. Chem., EUROBORON 3 Special Edition* **2005**, in press.
47. Frisch M. J., Trucks G. W., Schlegel H. B., Scuseria G. E., Robb M. A., Cheeseman J. R., Zakrzewski V. G., Montgomery J. A., Jr., Stratmann R. E., Burant J. C., Dapprich S., Millam J. M., Daniels A. D., Kudin K. N., Strain M. C., Farkas O., Tomasi J., Barone V., Cossi M., Cammi R., Mennucci B., Pomelli C., Adamo C., Clifford S., Ochterski J., Petersson G. A., Ayala P. Y., Cui Q., Morokuma K., Malick D. K., Rabuck A. D., Raghavachari K., Foresman J. B., Cioslowski J., Ortiz J. V., Baboul A. G., Stefanov B. B., Liu G., Liashenko A., Piskorz P., Komaromi I., Gomperts R., Martin R. L., Fox D. J., Keith T., Al-Laham M. A., Peng C. Y., Nanayakkara A., Gonzalez C., Challacombe M., Gill P. M. W., Johnson B., Chen W., Wong M. W., Andres J. L., Gonzalez C., Head-Gordon M., Replogle E. S., Pople J. A.: *Gaussian-98*, Revision A.7. Gaussian Inc., Pittsburgh (PA) 1998.
48. Farrugia L. J.: *ORTEP-3*; *J. Appl. Crystallogr.* **1997**, *30*, 565.